

# Workload Distribution Among Randomly Efficient Units

Zbigniew Domański

**Abstract**—We study how efficiently  $N$  interconnected units execute a common workload whose intensity grows. Units are characterized by quenched random thresholds of workload  $W$  they can support. A load  $W$  bigger than a given unit threshold breaks this unit irreversibly and triggers a sequence of other units failure. If  $W$  is applied progressively to the system, initial sequences of breaks develop in avalanches of failures and the system is pushed to the limit of its functionality. This limiting state of the system relates the critical load  $W_c$  and the number  $n_c < N$  of units that still are able to work. We employ computer simulations to study distributions of  $W_c$  and  $n_c$ . We show that in systems with uniformly random thresholds the critical  $W_c$  and  $n_c$  as well as the ratio  $W_c/n_c$  are distributed according to a skew-normal distribution with parameters fitted by power-law functions of  $N$ .

**Index Terms**—failure, multicomponent system, statistics, transfer rule, workload distribution.

## I. INTRODUCTION

**L**OAD-SHARING models are frequently applied to study efficiency and reliability of parallel systems. In this paper we consider a workload distribution among a large number of functionally identical units that perform a common task. When units become overloaded they fail and possibly trigger subsequent failures which reduce the system performance. An orchestrated sequence of overloaded units eventually leads to a catastrophic avalanche of failures. Such a catastrophe happens because systems subjected to an increasing load begin to fail when the internal workload exceeds the critical value of less reliable units. Then, the failure develops in a form of avalanche of simultaneously overloaded units. Precisely speaking, avalanches emerge when an increasing workload eliminates an unit from the system in such a way that the exclusion changes the internal workload pattern sufficiently to initiate the overload of other units. In consequence, the corresponding chain of failures provokes a wave of over-loadings. Avalanches of failures are frequently studied using so-called load transfer models as e.g. the Fibre Bundle Models (FBM) and Random Fuse Models [1], [2], [3], [4]. The FBM are particularly useful for study problems related to failure cascades in technological applications [5], [6], [7], [8], [9].

Our system is a set of units located at nodes of a lattice, see Fig. 1, and analysed using a Fibre Bundle Model methodology. In this work we limit our analysis to the case where each unit is characterized as working or overloaded (failed). We also assume that overloaded units are removed from the system. In our simulations, an ensemble of  $N$  components is subjected to a growing workload  $W$ , that systematically eliminates non-efficient units and initiates avalanches of failures.

Manuscript received July 30, 2019.

Z. Domański is with the Institute of Mathematics, Czestochowa University of Technology, Dabrowskiego 69, PL-42201 Czestochowa, Poland. (corresponding author e-mail: zbigniew.domanski@im.pcz.pl).

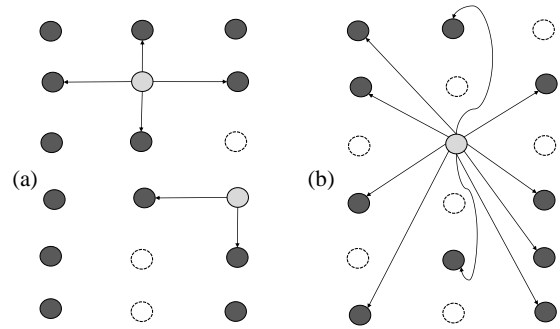


Fig. 1. Schematic diagram of a multiple-unit system. Disks represent units: black disks – working units, open circles – overloaded units, shade discs – just overloaded units with their workloads transferred to (a) neighbouring under-loaded units or (b) to all other units if the neighbourhood is inaccessible.

This means that when a unit fails, its workload is transferred to the other non-overloaded units. Obviously, such a transfer increases the probability of subsequent failures.

Due to structural imperfections and organisational factors, units' efficiencies are non uniform. We represent this non-uniformity by the unit-workload-thresholds. In simulations these thresholds are modelled by quenched random variables  $\{\sigma_i\}$ . Specifically, we assume that  $\{\sigma_i\}$  are distributed uniformly over the segment  $[\sigma_{min}, \sigma_{max}]$ .

In our simulations, a set of  $N$  units is subjected to a quasi-statically growing workload. Under the increasing  $W$  units begin to suffer from workloads approaching their load-thresholds and then fail. The workloads are redistributed through the system's units and together with the load already applied to the working units substantially accelerates new overloads. Thus, a cascade of overloads among units moves down the system performance and may eventually trigger a catastrophic avalanche of failures. Such critical avalanche develops when  $W$  reaches a specific, we call it critical, level  $W_c$ . This avalanche involves all still working units and the whole system breaks.

## II. SIMULATION FRAMEWORK

The rule of workload transfer is a fundamental factor of the model. Among many different rules there are two extreme ones: global load sharing (GLS) and local sharing (LLS) [10], [11], [12], [13], [14], [15], [16].

We transfer workloads from overloaded units according to a rule symbolized by arrows in Fig. 1. Let us consider  $i$ -th unit under the local workload  $w_i \leq \sigma_i$ . When  $W$  increases enough to attain locally  $w_i > \sigma_i$  then the  $i$ -th unit becomes over-loaded and stops working. At this circumstance  $w_i$  has to be undertaken by other units. At first attempt we

share  $w_i$  equally among nearest-neighbouring units if they are accessible. If no such neighbouring units the workload is uniformly distributed through entire set of under-loaded units. The first eventuality corresponds to the LLS transfer whereas the latter one reflects the GLS rule. Effectively such a workload-transfer rule represents a mixture of LLS and GLS rules. We call this transfer policy the mixed LLS-GLS rule. To some extent this rule corresponds to a recently reported strategy that helps to avoid a complete destruction of the system in presence of a cascade of failures [17].

As we have already mentioned, because of variable-range-load transfer, internal workloads are non-uniformly distributed. In consequence groups of units with workload accumulation emerge in the whole system. Growing internal load induces other overloads, after which each surviving unit sustains increasing workload. If the load transfer does not trigger further failures, a stable workloads' configuration emerges. This means that the given  $W$  is not sufficient to fail the entire system, and the applied  $W$  should increase.

In the simulations we apply a quasi-static procedure: if the system is in a stable configuration the applied  $W$  increases by an amount sufficient to overload the unit with the smallest  $(\sigma_i - w_i)$ . A series of increases in the value of applied workload gives  $W_c$ . In detail,  $W_c$  corresponds to a marginally stable configuration of the system, whereas  $W_c + \delta W$  provokes an avalanche of failures among all remaining units. By executing the quasi-static procedure we identify a workload  $W$  necessary to overload all the units and to get  $W_c$  and  $n_c$  describing the highest system's efficiency.

To determine the initial state of the system we assume unit's workload-thresholds  $\{\sigma_i\}$  are uniformly random. The main question is how these quenched random thresholds distributed uniformly over  $[\sigma_{min}, \sigma_{max}]$ , determine the resulting critical  $W_c$  and limiting number of units  $n_c$ . Based on results of simulations, we have found that coefficients of skewness of distributions of  $W_c/N$ ,  $n_c/N$  and  $W_c/n_c$  are negative and gathered data are correctly fitted by a three-parameter skew-normal distribution [18], [19], [20] defined by the density function

$$\psi_{SN}(x) = \frac{\text{erfc}\left(-\alpha \frac{x-\mu}{\sqrt{2}\sigma}\right)}{\sqrt{2\pi}\sigma} \exp\left[-\left(\frac{x-\mu}{\sqrt{2}\sigma}\right)^2\right] \quad (1)$$

where  $\mu$ ,  $\sigma$  and  $\alpha$  are respectively: location, scale and shape parameters.

### III. CRITICAL WORKLOAD AND MINIMAL NUMBER OF UNITS

Employing the mixed LLS-GLS rule symbolised in Fig. (1), we simulated a growing workload processes in systems of  $400 \leq N \leq 10000$  working units with quench thresholds  $\{\sigma_i\}$  distributed uniformly over  $[0, 1]$ . In order to achieve reliable estimates of  $W_c$  and  $n_c$  each simulation was executed  $10^4$  times. We have gathered ample data sets containing detailed information about applied workload ( $W$ ) and numbers of non-overloaded units ( $n$ ). We have used these  $W$ 's and  $n$ 's sets to determine corresponding statistics by merging  $W_c$  with number of units  $n_c$ . Some empirical estimators as *e.g.* the mean values, the standard deviations or the skewness have been taken into account as well.

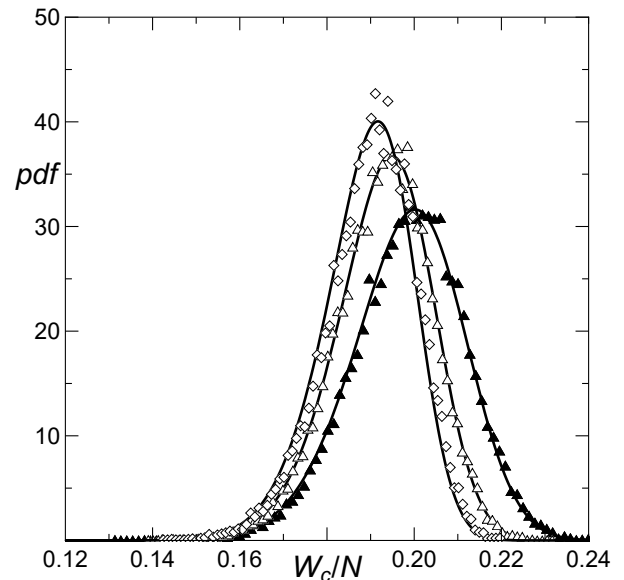


Fig. 2. Probability density of scaled critical workload  $W_c/N$  for systems with growing number of units: 900 (black triangles), 1600 (white triangles) and  $N = 2500$  (rhombus). Work-thresholds are distributed uniformly over  $[0, 1]$ . The solid lines represent skew normally distributed  $W_c/N$  with the parameters computed from the simulations. The results are obtained from  $10^4$  samples for each value of  $N$

The simulation framework presented in Section II enabled us to collect data sets of critical workloads  $W_c$  with corresponding minimal numbers of non-overloaded units  $n_c$  for various system sizes and uniformly distributed workload-thresholds. Then, based on these sets we have analysed resulting empirical probability density functions using different goodness-of-fit tests [21].

In Fig. (2) we show exemplary distributions of critical workload  $W_c$  scaled by corresponding numbers of units  $N$ . It turns out that  $\overline{W_c}/N$  are skew-normally distributed (1) with parameters related to  $N$  through power-law functions. Based on numerical data we fitted the mean  $\overline{W_c}/N$  and the standard deviation  $\text{st.dev}(W_c/N)$  to the following symbolic non-linear models

$$\overline{W_c}/N = a_m + \frac{b_m}{(\sqrt{N})^{c_m}} \quad (2)$$

$$\text{st.dev}(W_c/N) = a_s + \frac{b_s}{(\sqrt{N})^{c_s}} \quad (3)$$

where the parameters  $a_{m,s}, \dots, c_{m,s}$  are reported in Tab. (I) and the functions are displayed in Fig. (3). Formulas similar to (2) and (3) hold for  $\overline{n_c}/N$  as well. We do not display them here giving only the Fig. (4). We would like to underline that (2) and (3) reflect the mixed LLS-GLS rule applied to transfer overloads and the connectivity among units.

We have mentioned in Sec. (II) that the quasi-statically growing workload systematically reduces number of non-overloaded units and the system approaches critical state at which the maximal workload ( $W_c$ ) is executed by the reduced number of units ( $n_c$ ). This critical state is marginally stable and  $n_c$  is minimal because an additional overload triggers an avalanche that spans over the whole system. This means that  $W_c/n_c$  is directly related to an average density of workload. In Fig. (5) we display empirical distributions of  $W_c/n_c$  for

TABLE I  
 PARAMETERS OF ESTIMATED MEAN  $\bar{W}_c/N$  (2) AND STANDARD  
 DEVIATION  $\sigma(W_c)/N$  (3), FOR SYSTEMS WITH GROWING NUMBER OF  
 UNITS

Parameter	Estimate	Standard Error	Confidence Interval
$a_m$	0.125727	0.013307	(0.006034, 0.008303)
$b_m$	0.179412	0.003116	(0.172364, 0.186461)
$c_m$	0.266343	0.049344	(0.154720, 0.377966)
$a_s$	0.007168	0.000502	(0.785590, 0.800570)
$b_s$	0.245501	0.060994	(0.107522, 0.383480)
$c_s$	1.112720	0.100209	(0.886030, 1.339410)

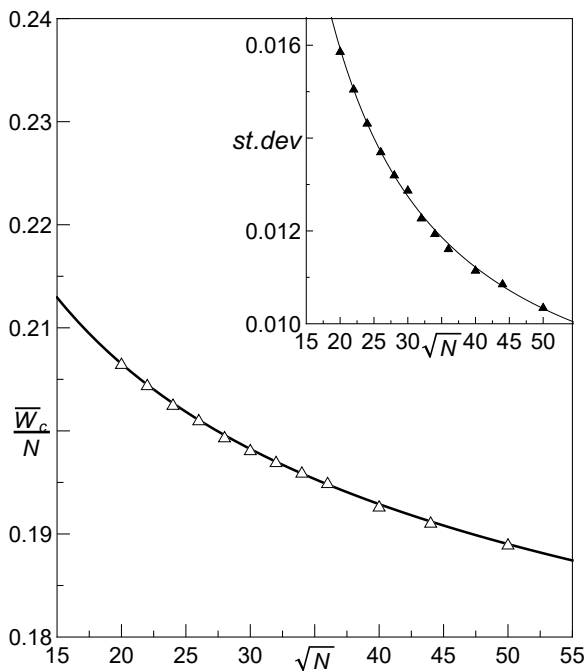


Fig. 3. Mean and standard deviation (inset) of critical workload  $W_c$  for systems with growing number of units. Solid lines are drawn using (2) and (3), respectively.

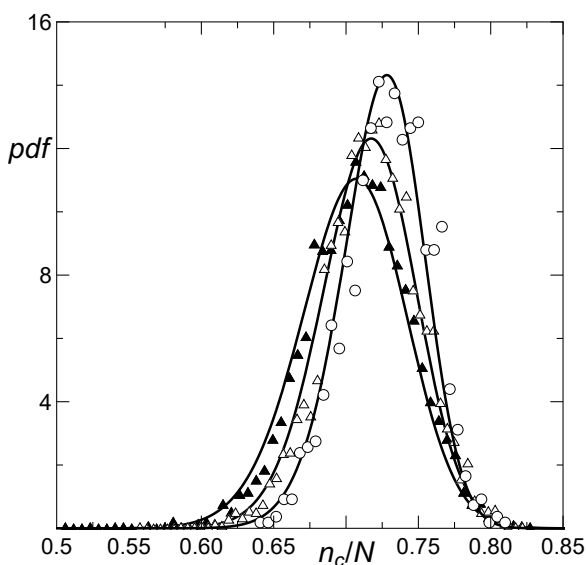


Fig. 4. Distributions of scaled minimal number of channels  $n_c/N$  for systems with  $N = 3600$  (white disks),  $N = 2500$  (white triangle) and  $N = 1600$  units. The solid lines represent skew normally distributed  $n_c/N$  with the parameters computed from the simulations. The results are obtained from  $10^4$  samples for each value of  $N$

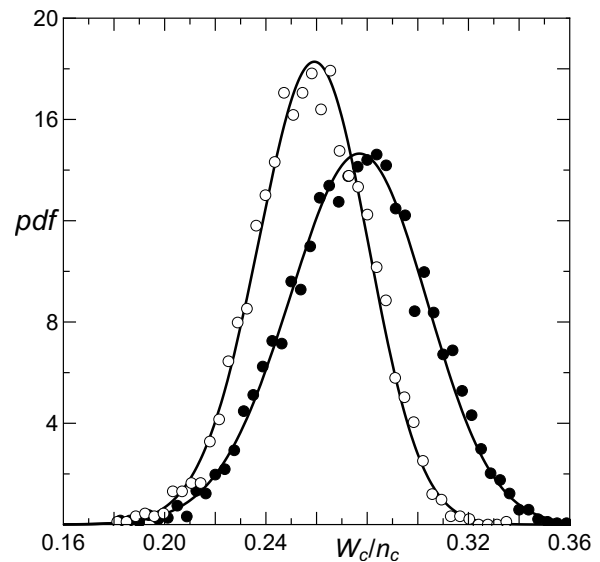


Fig. 5. Empirical probability density of  $W_c/n_c$  for systems with 3600 units (white disks) and 1600 units (black disks). The solid lines are drawn using (1) with parameters estimated from the simulations. Sample size is  $10^4$ .

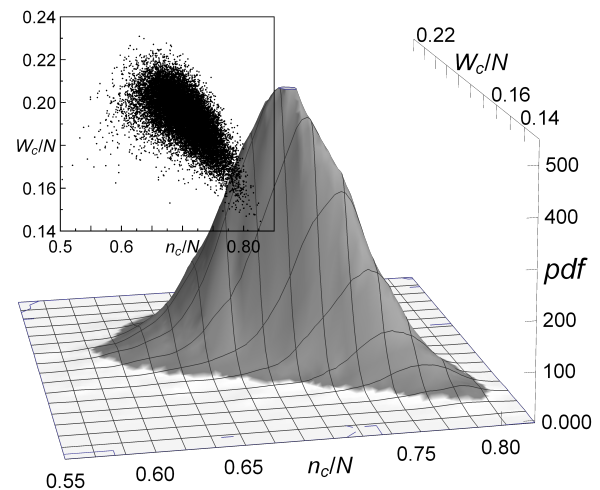


Fig. 6. Empirical joint probability density functions of  $n_c/N$  and  $W_c/N$  for systems with 1600 units. Sample size is  $2.5 \times 10^4$ .

systems with  $N_1 = 3600$  and  $N_2 = 1600$  units. It is clearly seen that bigger  $N$  corresponds to lower value of  $\bar{W}_c/n_c$ . Such a behaviour of  $\bar{W}_c/n_c$  may also be deduced from Figs. (2) and (4). These figures show that with growing  $N$  the mean critical workload  $\bar{W}_c/N$  decreases whereas  $\bar{n}_c/N$  increases. (5). Obviously, a quantitative analysis requires data displayed in Fig. (5). We extend properties of relation between critical workload and number of non-overloaded units by presenting an example of empirical joint probability density function of  $n_c/N$  and  $W_c/N$ . This exemplary pdf related to the system with  $N = 1600$  units is presented in Fig. (6). We have built it by joining, sample by sample, critical workloads  $W_c/N$  with corresponding  $n_c/N$ . The inset in this Figure illustrates the shape of joint pdf support. The Pearson coefficient  $r$  related to presented distributions equals to  $r = -0.639$ .

Now we compare  $W_c$  and  $n_c$  related to systems whose units are associated with nodes of the square lattice with periodic boundary condition to the same quantities but related

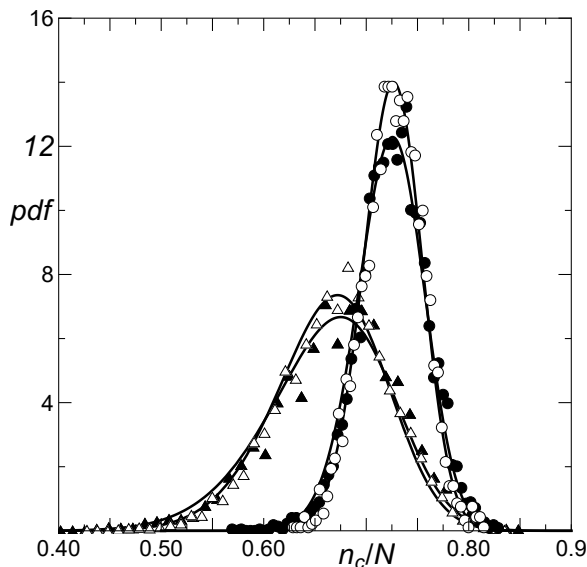


Fig. 7. Distributions of scaled minimal number of units  $n_c/N$  for systems with  $N = 400$  (triangles) and  $N = 3600$  (disks) units. White triangles and white disks represent systems located on a square lattice with periodic boundary conditions whereas the black plot-marks belong to data from systems where no periodicity on boundaries takes place. The solid lines are skew normally distributed  $n_c/N$  with the parameters computed from simulations. The results are obtained from  $10^4$  samples for each data set.

to units in presence of open boundaries of the underlying lattice. From the topological point of view the former case corresponds to the nodes lying on a torus. Periodic boundary guarantees a perfect neighbourhood for all the units. This is not the case when open boundary are present, i.e. the system suffers from smaller number of links among units on the border and thus the local load transfer is less efficient. This reduced local load transfer affects at most a fraction of the order  $1/\sqrt{N}$  of units and can be neglected for systems with  $N \gg 1$ . Figure (7) displays corresponding data.

#### IV. FINAL REMARKS

We have examined task distributions among functionally identical units subjected to a quasi-statically increasing workload. We have characterised units by quench random thresholds distributed uniformly and employed the mixed LLS-GLS rule to transfer workload from overloaded units to non-overloaded ones. Based on results of simulations we have shown that the experimental distributions of the critical load  $W_c$ , minimal number of non-overloaded units  $n_c$  as well as the local-workload intensity  $W_c/n_c$  follow the skew-normal distribution. By fitting discrete distributions we have found that:

- (i) for uniformly random workload thresholds expected maximal load supported by the system depends mainly on the rule of workload transfer, i.e.  $W_c/N \sim N^{-0.133}$  for the mixed LLS-GLS rule examined in this work,  $W_c/N \sim 1$  for the GLS rule and  $W_c/N \sim (\log N)^{-0.41}$  when the LLS rule is applied [8],
- (ii) minimal numbers of non-overloaded units  $n_c$  are skew-normally distributed when the mixed LLS-GLS rule is used in contrast to normally distributed  $n_c$  when the LLS rule is applied.

Even that the mixed LLS-GLS rule of workload transfer is chosen arbitrary we observe that this rule represents

a reasonable compromise between the LLS and the GLS rules, however. The mixed LLS-GLS rule distributes locally-accumulated overload among neighbouring units if they are accessible and the entire system is engaged only when such a neighbourhood is already destroyed.

#### REFERENCES

- [1] A. Hansen, P.C. Hemmer, and S. Pradhan, "The Fiber Bundle Model: Modeling Failure in Materials," Weinheim, Wiley-VCH, 2015.
- [2] F. Kun, F. Raischel, R.C. Hidalgo, and H.J. Herrmann, "Extensions of fibre bundle models," in *Modelling Critical and Catastrophic Phenomena in Geoscience, Lecture Notes in Physics*, P. Bhattacharyya and B.K. Chakrabarti, Eds, vol. 705, Berlin: Springer 2006, pp. 57-92.
- [3] M.J. Alava, P.K.V.V. Nukala, and S. Zapperi, "Statistical models of fracture," *Adv. In Physics*, vol. 55, pp. 349-476, April 2006.
- [4] D. Cohen, P. Lehmann and D. Or, "Fiber bundle model for multiscale modeling of hydromechanical triggering of shallow landslides," *Water Resources Res.*, vol. 45, W10436, Oct. 2009.
- [5] Z. Bertalan, A. Shekhawat, J.P. Sethna, and S. Zapperi, "Fracture strength: Stress concentration, extreme value statistics and the fate of the Weibull distribution," *Phys. Rev. Applied*, vol. 2, id. 034008, Sept. 2014.
- [6] C. Manzato, A. Shekhawat, P. K. V. V. Nukala, M. J. Alava, J. P. Sethna, and S. Zapperi, "Fracture Strength of Disorder Media: Universality, Interactions, and Tail Asymptotics," *Phys. Rev. Lett.*, vol. 108, id. 065504, Feb. 2012.
- [7] J. Knudsen and A.R. Massih, "Breakdown of disordered media by surface loads," *Phys. Rev. E*, vol. 72, id. 036129, Sept. 2005.
- [8] S. Zapperi, P. Ray, H.E. Stanley, and A. Vespignani, "Analysis of damage clusters in fracture processes," *Phys. A*, vol. 270, pp. 57-62, Aug. 1999.
- [9] Z. Domanski, T. Derda and N. Sczygiol, "Critical Avalanches in Fiber Bundle Models of Arrays of Nanopillars," *Lecture Notes in Engineering and Computer Science: the International MultiConference of Engineers and Computer Scientists 2013*, 13-15 March, 2013, Hong-Kong, pp. 765-768.
- [10] Z. Domanski, "Damage Statistics in Progressively Compressed Arrays of Nano-pillars", *Eng. Letters*, vol. 27, no. 1, pp. 18-23, February 2019.
- [11] H. Daniels, "The statistical theory of the strength of bundles of threads I," *Proc. Royal. Soc. A*, vol. 83, pp. 405-435, 1945.
- [12] B. Coleman, "Time dependence of mechanical breakdown in bundles of fibers I. Constant total load," *J. Appl. Phys.*, vol. 28, pp. 10581064, 1957.
- [13] B. Coleman, "Time dependence of mechanical breakdown in bundles of fibers II. The infinite ideal bundle under linearly increasing loads," *J. Appl. Phys.*, vol. 28, pp. 10651067, 1957.
- [14] R.C. Hidalgo, Y. Moreno, F. Kun, and H.J. Herrmann, "Fracture model with variable range of interaction," *Phys. Rev. E*, vol. 65, id. 046148, April 2002.
- [15] D. Wang, Ch. Jiang and Ch. Park, "Reliability analysis of load-sharing systems with memory", *Lifetime Data Anal.*, vol. 25, pp. 341-360, 2019.
- [16] T. Derda, "Analysis of damage processes in nanopillar arrays with hierarchical load transfer," *J. Appl. Math. Comput. Mech.*, vol. 15(3), pp. 27-36, 2016.
- [17] Z. Domanski, T. Derda and N. Sczygiol, "Statistics of critical avalanches in vertical nanopillar arrays," in *Transactions on Engineering Technologies. Lecture Notes in Electrical Engineering*, G.C. Yang, S.I. Ao, X. Huang, O. Castillo, Eds., vol. 275, Dordrecht: Springer, 2014, pp. 1-11.
- [18] C.E. La Rocca, H.E. Stanley and L.A. Branunstein, "Strategy in interdependent networks to avoid the complete destruction of the system in the presence of a cascade of failures", *Physica A: Statistical Mechanics and its Applications*, vol. 508, pp. 577-583, 2018.
- [19] A. OHagan, and T. Leonard, "Bayes estimation subject to uncertainty about parameter constraints," *Biometrika*, vol. 63, 201-202, April 1976.
- [20] A. Azzalini and A.R. Massih, "A class of distributions which includes the normal ones," *Scand. J. Statist.*, vol. 12, pp. 171-178, June 1985.
- [21] A. Azzalini, "The Skew-Normal and Related Families," Cambridge: Cambridge University Press, 2013.
- [22] T.B. Arnold and J.W. Emerson, "Nonparametric Goodness-of-Fit Tests for Discrete Null Distributions," *The R Journal*, Vol. 3/2, pp. 34-39, December 2011.